Short Note

Shear-Wave Velocity Structure of the Koyna–Warna Region in Western India Using Ambient Noise Correlation and Surface-Wave Dispersion

by Sunil Rohilla,[*] N. Purnachandra Rao,[*] Peter Gerstoft, D. Shashidhar, and H. V. S. Satyanarayana

Abstract   The Koyna–Warna region is a premier site of reservoir-triggered seismicity in the Deccan volcanic province of western India. In the present study, shear-wave velocity structure of this region down to a depth of 10 km is estimated using the ambient noise correlation technique with data from a network of 11 seismic broadband stations. Asymmetric Green's functions are obtained that are suggestive of an anisotropic distribution of noise sources in the Indian subcontinent. Cross correlation of continuous noise data of 12 months duration, recorded on the vertical components, enables computation of group velocity dispersion curves from the Green's functions. This is supplemented by Rayleigh waves from local earthquakes, which, in addition to those from noise data, are inverted for the shear-wave velocity structure using the multiple-filter technique. The study reveals on an average, a 0.8 km thick basaltic layer of the Deccan traps with a shear-wave velocity of about 3.0 km/s on the eastern side of the escarpment. A low-velocity, possibly weathered granitic layer with a velocity of 3.3 km/s is found below the traps and is underlain by the granitic basement with a velocity of 3.6 km/s. Except for the surface topographic undulation, the velocity structure in this region, down to 10 km, is similar on either side.

Introduction

The Koyna–Warna region in the Western Ghats of India is a globally well-known site of reservoir-triggered seismicity (Gupta *et al.*, 1969; Gupta and Rastogi, 1976; Gupta, 2002). Over the past 50 yrs the region has experienced 22 $\mathbf{M} \geq 5$ earthquakes. The seismicity followed the impoundment of the Koyna Dam in 1962 and subsequently the Warna dam situated about 25 km southeast in 1985. Since 1993–1994, a southward shift of seismicity has been observed in the Warna region (Rastogi *et al.*, 1997). The area is covered by Deccan traps, mainly comprising volcanic basalt, with thickness estimated to vary from 1 to 2 km (Gubin, 1969). According to King (1962), the maximum thickness of basalt flow in the Deccan traps is about 2 km. A study of dispersion of short-period Love waves (Tandon, 1973) shows that the average thickness of the Deccan traps in the Koyna region is 1.25 km, with the *P*-wave velocity varying from 4.7 to 5.2 km/s in the basaltic layer and from 5.85 to 6.5 km/s in the granitic layer. Deep seismic sounding studies in the Koyna region (Kaila *et al.*, 1981) revealed some finer

structures of the Deccan traps and the basement rock, down to the Moho depth. The trap thickness varies from 1.5 km on the west coast to about 0.4 km toward the east. The *P*-wave velocity in the trap layer varies from 4.7 to 4.9 km/s and is 5.9 to 6.1 km/s in the granitic layer. Deep electric sounding (Kailasam *et al.*, 1976) shows that the thickness of traps at Guhagaron on the west coast is 0.82 km, whereas it is 1 km at Koyna. Recent drilling studies by the Council of Scientific and Industrial Research (CSIR)-National Geophysical Research Institute at Rasati, about 2.5 km south of the Koyna dam, show the basalt to be 933 m thick with a granitic basement immediately beneath it (Rao *et al.*, 2013; Roy *et al.*, 2013).

In the present study, we use the ambient noise correlation technique to estimate the shear-wave velocity structure down to about 10 km depth in the Koyna–Warna region. Rayleigh waves are generated from the vertical components by the correlation of continuous seismic traces between pairs of seismic stations. The cross-correlation functions are used to obtain the dispersion curves and subsequently a 1D shear-wave velocity model of the region. Also, surface waves of some local earthquakes of magnitude greater than 4.0 are

---

*Also at Academy of Scientific and Innovative Research, CSIR-National Geophysical Research Institute, Hyderabad, India.
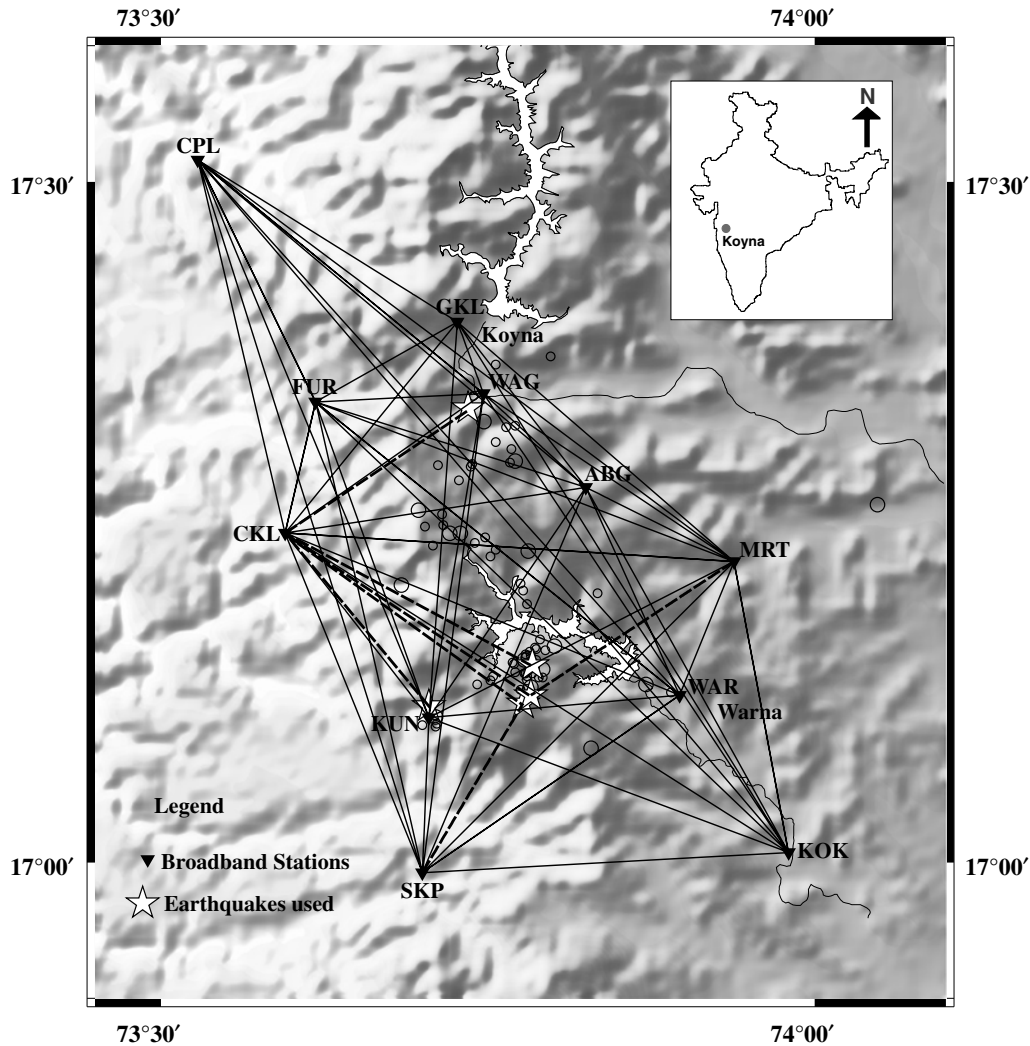
Figure 1. The Koyna–Warna region in western India, comprising the Deccan trap cover and indicating the network of 11 seismic broadband stations (inverted triangles), along with the station codes and seismicity ($\mathbf{M} \geq 3$) of the region in the last seven years. The inset shows the location of the Koyna–Warna region. The lines joining the station pairs represent the ray paths of the Green's functions, whereas the thick dashed lines show the ray paths between earthquake epicenters and the seismic stations that were used for dispersion analysis.

analyzed to study the dispersion characteristics, supplementing the results of ambient noise correlation.

Data and Analysis

In the present study, continuous waveform data from a seismic network of 11 broadband stations in the Koyna–Warna region of western India (Fig. 1) are used. Continuous time series of 12 months duration with a sampling interval of 0.01 s recorded on the vertical component of each station are cross correlated with that of every other station.

Noise Cross Correlation

Ambient noise is a random process generated by wind, human activities, oceanic disturbance, etc. Ocean waves are the main source of seismic ambient noise in the 5–10 s period range (Longuet-Higgins, 1950). Assuming that noise sources

are distributed homogeneously around the station, the cross correlation of the continuous noise data of one station with respect to the other yields the Green's function (Lobkis and Weaver, 2001) corresponding to the Rayleigh and Love waves (Campillo and Paul, 2003; Shapiro and Campillo, 2004; Sabra *et al.*, 2005). Ambient noise correlation was successfully used to obtain tomographic images of the western part of the United States (Shapiro *et al.*, 2005; Gerstoft *et al.*, 2006). The same technique was applied to the south Indian shield region to get the velocity structure beneath the Dharwar craton (Borah *et al.*, 2014).

Cross correlation, C, is computed from the observed noise field $v_A(r_A, t)$ and $v_B(r_B, t)$ at locations r_A and r_B by integration over the entire observation period T as

$$C(A, B, t) = \int_0^T v_A(r_A, \tau) v_B(r_B, t + \tau) d\tau. \quad (1)$$
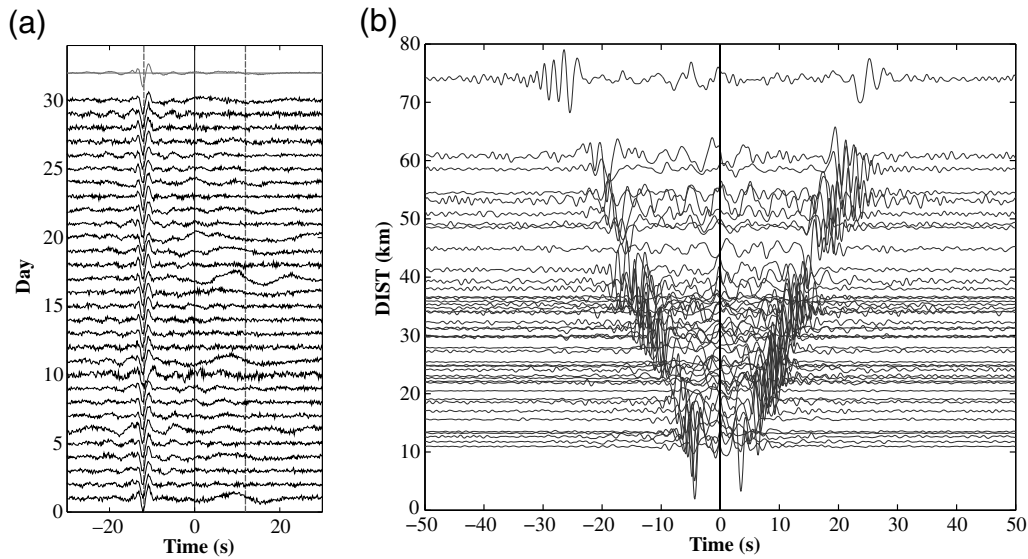
Figure 2. (a) Daily correlations of ambient noise between stations SKP and MRT, indicating consistent arrival times of the empirical Green's functions, which are stacked (the gray trace at the top); the two vertical dashed lines correspond to a velocity of 2.0 km/s. Asymmetric Green's functions indicate directivity of noise sources, mainly from the Indian Ocean in the south. (b) Empirical Green's functions from the correlation of ambient noise, with respect to station separation (DIST) in the Koyna–Warna region.

The time-domain Green's function generated after the cross correlation will have the causal and anticausal parts, which are given by the relation

$$\frac{d(C_{AB}(t))}{dt} \equiv -g(r_A, r_B, t) + g(r_B, r_A, -t). \qquad (2)$$

In this study, continuous data for a period of one year (2011) has been used to compute the cross correlation for each station pair of the network (Fig. 1). Individual segments of 3600 s are selected for cross correlation. The seismograms are band-pass filtered between 0.33 and 50 s and resampled at 0.1 s. For removal of earthquakes, the amplitude is clipped to a threshold value (Gerstoft *et al.*, 2006). Cross correlation of traces of each station pair is computed for each month of the year, and then the resulting time lag traces are stacked to get the Green's function. Figure 2a shows the daily correlations at station pair SKP–MRT, which are subsequently stacked to obtain the Green's function. Figure 2b shows the shift in arrival times of the Green's functions as a function of station separation in kilometers. Figure 3a–c shows examples of Green's functions generated in different frequency ranges for the station pair SKP–MRT, which look similar to a conventional local earthquake surface wave (Fig. 3d). For the Koyna–Warna region, the Green's functions are predominantly one sided (Fig. 2a), with noise likely generated from the south at the nearest coastal region. In fact, most seismic station pairs of the entire Indian plate region have produced one-sided Green's functions, as demonstrated by Rao *et al.* (2009), who attributed this to the anisotropic distribution of noise sources primarily due to the ocean wave disturbance from the Indian Ocean in the southwest. The correlation function for each station pair is used to generate the group velocity dispersion curve of Rayleigh waves, which is inverted

to obtain the shear-wave velocity structure corresponding to the region between the two stations. A similar analysis is also carried out using data of five local earthquakes of $\mathbf{M} \geq 4.0$ in the Koyna–Warna region (Table 1), which yielded comparable results. Figure 3d shows an example of the event data used.

Inversion of Surface Waves from Ambient Noise

The Rayleigh-wave Green's functions obtained by cross correlation of ambient noise at each station pair are used to estimate group velocity dispersion curves using the multiple-filter technique (Dziewonski *et al.*, 1969). The fundamental mode dispersion curves are picked in the period range of 0.33–10 s. The parameters that are required for the estimation of group velocity are the event and the station locations, distance between event and station, origin time, and azimuth from event to station. The estimated group velocities are inverted for a 1D shear-wave velocity structure using the inversion scheme of Herrmann (1987) and Russell (1987). The method uses a stochastic damped least-squares inversion that minimizes the misfit with the observations in an L2 norm. The technique allows for the evaluation of partial derivatives of the group velocities with respect to the shear and compressional velocities and the densities of the layers. Model parameters are perturbed from the initial guess and fit to the observed values. The starting model for the inversion is considered as a half-space earth model with four layers having a constant velocity of 3 km/s, which generally converges to the true model after a few iterations. The velocity structure is estimated for each station pair using the group velocity dispersion data. The regions on either side of the escarpment are dealt with separately because the elevation of the stations is low on the western side and high on the eastern side. The average velocity structure is obtained

(a)

(b)

(c)

(d)
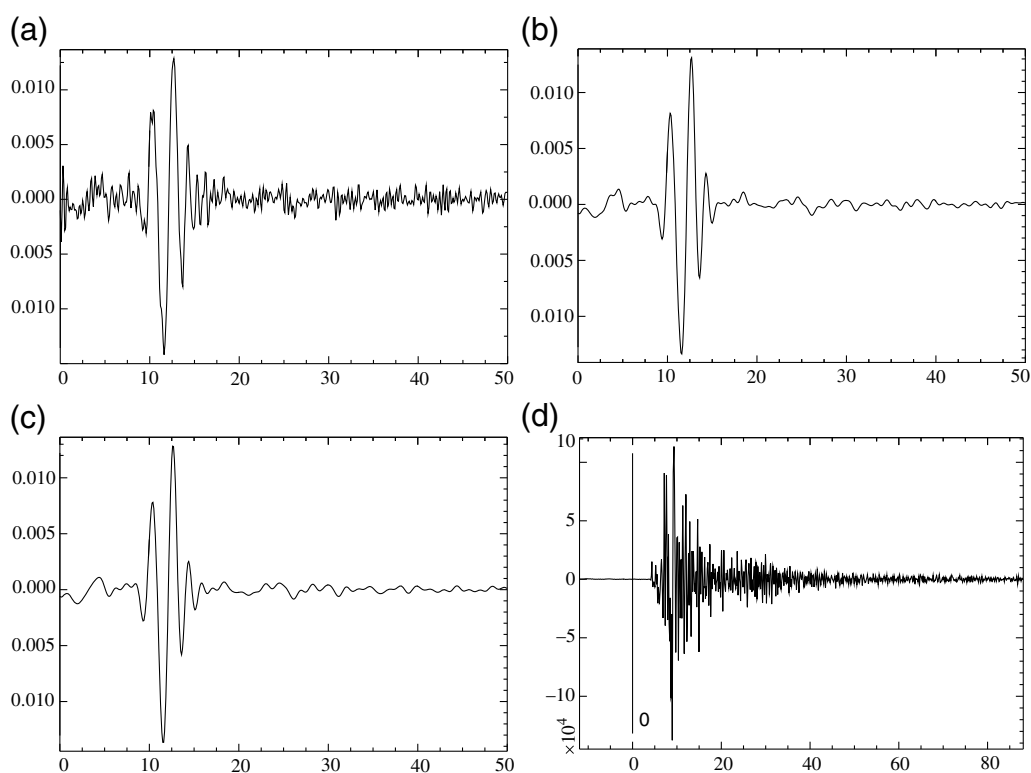
Figure 3. Example of a cross-correlation function generated for five months for the station pair SKP–MRT in the period ranges of (a) 0.02–3 Hz, (b) 0.02–1 Hz, and (c) 0.09–0.8 Hz. (d) The peak arrival time of the Rayleigh wave is similar to that of the conventional surface wave from local earthquakes in the region.

by inversion of the dispersion curves along all the paths in both the regions. Figure 4a,b shows the best-fit dispersion curves obtained for the eastern and western sides of the escarpment, respectively.

Inversion of Surface Waves from Earthquakes

A similar analysis is carried out for inversion of surface waves from the five largest recent local earthquakes recorded on seven stations. The fundamental mode Rayleigh-wave dispersion curves are picked in the 0.33–10 s period range. As in the case of ambient noise data, a simple four-layered model with a constant shear-wave velocity of 3.0 km/s is used as the starting model. The best-fit dispersion curve is obtained from inversion (Fig. 4c) to get an average velocity model.

Results and Discussion

Velocity Structure from Ambient Noise

Velocity models are obtained along the paths between each station pair indicated in Figure 1. On the eastern side, the thickness of the top Deccan basalt layer is estimated to be about 0.8 km, with an average shear-wave velocity of 3.0 km/s. This is underlain by a layer down to 2 km, with an average velocity of 3.3 km/s. The *S*-wave velocity in the granitic basement further below is 3.6 km/s (Fig. 5a). On the western side of the escarpment, the shear-wave velocity of the top layer is 3.3 km/s (Fig. 5b). This is higher than the velocity of the top layer on the eastern side, which is mostly the topographic high and in fact corresponds to the velocity of the second layer on the eastern side. It appears that the thickness of the top basalt layer on the western side cannot

Table 1

Local Earthquakes of Magnitude Greater than 4.0 Recorded by the Koyna Network (Fig. 1), Used in the Present Study

Date (yyyy/mm/dd)	Origin Time (hh:mm:ss.ss)	Latitude (°N)	Longitude (°E)	Depth (km)	Magnitude
2007/08/20	19:15:54.5	17.145	73.784	3.6	4.3
2007/11/24	10:57:47.1	17.111	73.705	3.1	4.8
2009/11/14	13:34:34.8	17.117	73.777	3.2	4.0
2009/12/12	11:51:24.8	17.129	73.783	4.7	5.1
2012/04/14	05:27:41.00	17.334	73.735	11.6	4.8
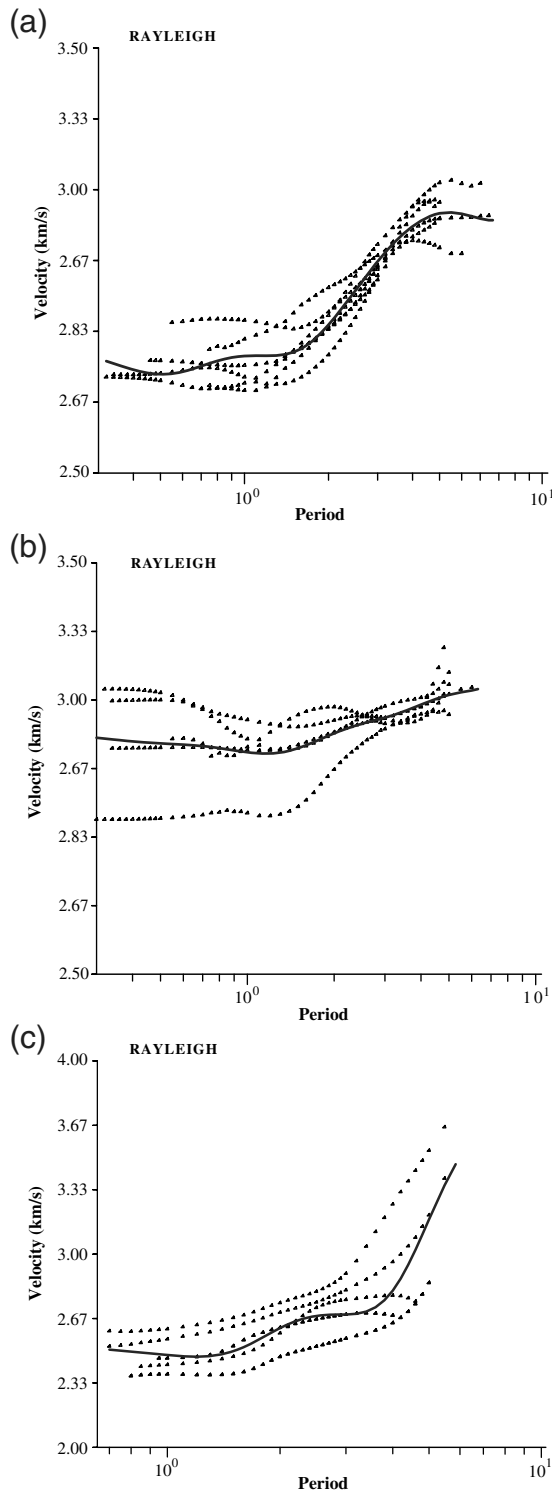
Figure 4. Dispersion curves and best fit corresponding to (a) all the station pairs on the eastern side, (b) all the station pairs on the western side of the escarpment, and (c) for the five large recent earthquakes. The thick lines show the best fit theoretical curves, whereas the dots are the observed data points. Station pairs for the eastern side are ABG–GKL, KOK–ABG, KOK–WAG, KOK–GKL, MRT–GKL, MRT–WAG, WAR–ABG, and WAR–WAG, and for the western side they are CKL–CPL, FUR–CPL, KUN–CPL, KUN–FUR, and SKP–FUR. The abscissa shows the wave period up to 10 s, and the coordinate is the group velocity of Rayleigh waves.

possibly be resolved by the present approach with the available data. However, the velocity structure from the second layer onward seems to be quite similar on both sides. The average velocity model, which is well resolved on the eastern side, is shown in Table 2.

Velocity Structure from Earthquake Data

Conventional surface-wave dispersion analysis is carried out using selected earthquake data to compliment the results of velocity structure using ambient noise data. The results obtained from inversion are quite similar, although deviations are expected in view of variations in the paths, focal depths, and lateral heterogeneities in the structure. The thickness of the basaltic layer is about 1.0 km. The average velocity model estimated from earthquake data is shown in Table 3. As the epicentral distances for local earthquakes in the Koyna–Warna region is very small, it is apparent that the surface-wave dispersion analysis can only resolve the upper few kilometers.

Error Analysis Using Bootstrap Technique

The similarity of velocity models derived from each individual baseline, as seen in Figure 5a,b, demonstrates the robustness of the overall inversion. The delineation of the top basalt layer and of the upper crustal layer is clear, although the scatter in the layer parameters increases with depth. Also, the resolution of thickness of the top layer on the western side is uncertain, possibly due to its low value, which is largely due to low topography.

To further ascertain the error limits of the velocity model and to estimate the confidence level of the results, the bootstrap technique (Efron and Tibshirani, 1986) is applied. In this method, a number of samples equal to the total number of dispersion curves is drawn randomly from the master set and inverted each time. Each set would be slightly different from the others because some samples are repeated whereas others are omitted, with the total number remaining the same. The uncertainties in the results of inversion are given by the scatter in the various models obtained. The confidence limits for the shear-wave velocity structure obtained on the eastern side are depicted in Figure 6. It is important to note that the model is well constrained, particularly in the top two layers depicting the Deccan basalt and the weathered upper granitic basement; this is seen in the inversions from individual baselines in Figure 5a,b.

Conclusions

The average Deccan trap thickness in the Koyna–Warna region is estimated as 0.8 km, with a shear-wave velocity of 3 km/s underlain by a layer with a velocity of 3.3 km/s, which probably represents a weathered granitic layer. A massive granite-gneissic basement is observed beneath the weathered part with a shear-wave velocity of 3.6 km/s. The basalt thickness on the western side is not so well resolved because

(a)

(b)
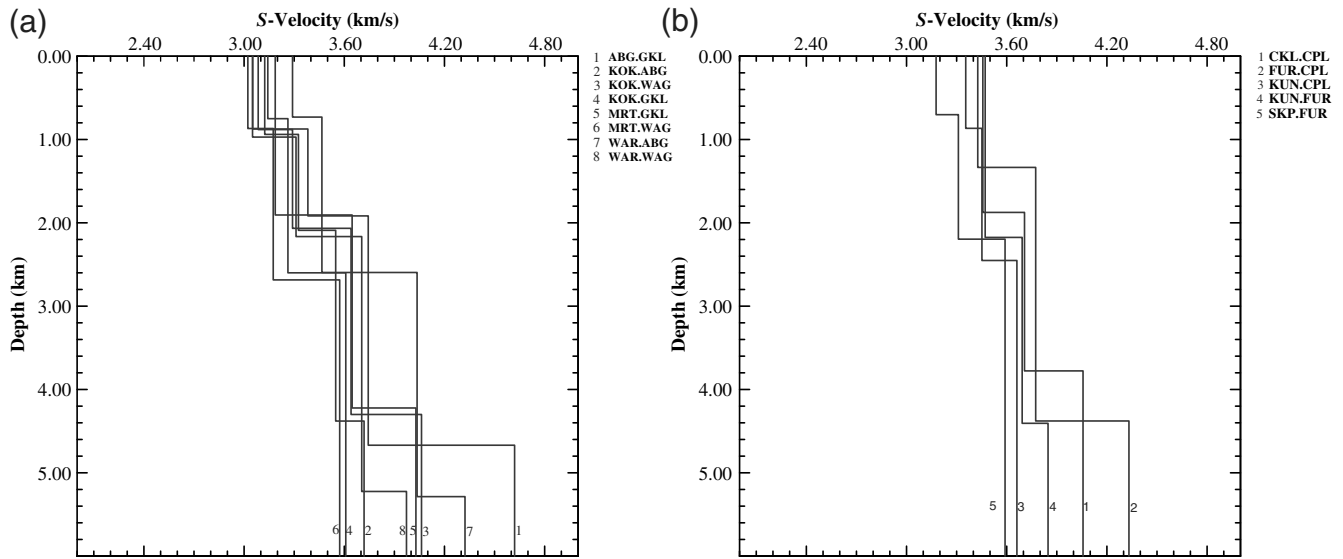
Figure 5.   The shear-wave velocity models obtained by inverting the dispersion curves along each station pair on (a) the eastern and (b) the western side of the escarpment. Numbers are given to each station pair.

Table 2

The Best Shear-Wave Velocity Model from the Ambient Noise Correlation Study Using All the Dispersion Curves on the Eastern Side of the Escarpment

Depth (km)	Shear Velocity (km/s)
0.0	3.0
0.8	3.3
2.4	3.6
6.5	3.9

Table 3

The Average Velocity Model Generated Using Group Velocity Dispersion from Earthquake Data

Depth (km)	Shear Velocity (km/s)
0.0	2.9
1.0	3.1
2.1	3.6

Figure 6.   Shear-wave velocity structure of the Koyna–Warna region on the eastern side of the escarpment and the uncertainty limits in velocity and layer thickness obtained by the bootstrap method. The thick line shows the mean value, whereas the light lines show the deviation from the mean.

there are fewer station paths than that required to resolve a thin layer. High-frequency ambient noise tomography studies would shed light on the precise structure of the region.

Data and Resources

A network of 11 broadband digital seismographs (Fig. 1) is operated by the Council of Scientific and Industrial Research-National Geophysical Research Institute, Hyderabad, India. The seismic stations cover an area of about 20×30 km^2. Ambient noise data of 12 months duration for the year 2011 are analyzed to estimate the noise correlation function. The sensor modelss are REF TEK 151-120A with a

120 s 50 Hz frequency band and CMG-3ESP with a 30 s 50 Hz frequency band. The data has a sampling frequency of 100 Hz. The elevation of stations from the mean sea level varies from 26–930 m. Some plots were made using Generic Mapping Tools version 4.5.7 (www.soest.hawaii.edu/gmt, last accessed January 2012; Wessel and Smith, 1998).

Acknowledgments

ment of India. The comments of reviewers and the Associate Editor are gratefully acknowledged because they have greatly helped in improving the manuscript.

References

Borah, K. J., S. S. Rai, K. S. Prakasam, S. Gupta, K. Priestley, and V. K. Gaur (2014). Seismic imaging of crust beneath the Dharwar craton, India, from ambient noise and teleseismic receiver function modelling, *Geophys. J. Int.* **197,** no. 2, 748–767.

Campillo, M., and A. Paul (2003). Long-range correlation in the diffuse seismic coda, *Science* **299,** 547–549.

Dziewonski, A., S. Bloch, and M. Landsiman (1969). A technique for the analysis of transient seismic signal, *Bull. Seismol. Soc. Am.* **97,** 198–207.

Efron, B., and R. Tibshirani (1986). Bootstrap methods for standard errors, confidence intervals and other measures of statistical accuracy, *Stat. Sci.* **1,** 54–77.

Gerstoft, P., K. G. Sabra, P. Roux, W. A. Kuperman, and M. C. Fehler (2006). Green's function extraction and surface-wave tomography from microseism in southern California, *Geophysics* **71,** S123–S131.

Gubin, I. E. (1969). Koyna earthquake of 1967, *Bull. Inst. Seism. Earthq. Eng.* **6,** 45–62.

Gupta, H. K. (2002). A review of artificial reservoir triggered earthquakes with special emphasis on earthquakes in Koyna, India, *Earth Sci. Rev.* **58,** 279–310.

Gupta, H. K., and B. K. Rastogi (1976). *Dams and Earthquakes*, First Ed., Elsevier Scientific Publishing Company, Amsterdam, The Netherlands, 372 pp.

Gupta, H. K., H. Narain, B. K. Rastogi, and I. Mohan (1969). A study of the Koyna earthquake of December 10, 1967, *Bull. Seismol. Soc. Am.* **59,** 1149–1162.

Herrmann, R. B. (1987). *Computer Programs in Seismology, User's Manual*, St. Louis University, St. Louis, Missouri.

Kaila, K. L., P. R. K. Murthy, V. Rao, and G. E. Kharatchko (1981). Crustal structure from deep seismic soundings along the Koyna II (Kelsi-Loni) profiles in the Deccan Trap area, India, *Tectonophysics* **73,** 365–384.

Kailasam, L. N., A. G. B. Reddy, J. M. V. Rao, K. Satyamurthy, and B. S. R. Murthy (1976). Deep electrical resistivity soundings in the Deccan Trap region, *Curr. Sci.* **45,** 9–13.

King, L. C. (1962). *The Morphology of the Earth*, Oliver and Boyd, Edinburgh, Scotland.

Lobkis, O. I., and R. L. Weaver (2001). On the emergence of the Green's function in the correlations of a diffuse field, *J. Acoust. Soc. Am.* **110,** 3011–3017.

Longuet-Higgins, M. S. (1950). A theory of the origin of microseisms, *Phil. Trans. Roy. Soc. London* **243,** 2–36.

Rao, N. P., P. Gerstoft, J. Zhang, D. Srinagesh, and M. Ravi Kumar (2009). Ambient seismic noise correlation in the Himalayan foothills for crustal structure, *AGU Fall Meeting*, San Francisco, California, 14–18 December 2009.

Rao, N. P., S. Roy, and K. Arora (2013). Deep scientific drilling in Koyna, India—Brainstorming workshop on geological investigations 19–20 March 2013, *J. Geol. Soc. India* **81,** 722–723.

Rastogi, B. K., R. K. Chadha, C. S. P. Sarma, P. Mandal, H. V. S. Satyanarayana, I. P. Raju, N. Kumar, C. Satyamurthy, and A. N. Rao (1997). Seismicity at Warna reservoir (near Koyna) through 1995, *Bull. Seismol. Soc. Am.* **87,** no. 6, 1484–1494.

Roy, S., N. P. Rao, V. V. Akkiraju, D. Goswami, M. Sen, H. K. Gupta, B. K. Bansal, and S. Nayak (2013). Granitic basement below Deccan Traps unearthed by drilling in the Koyna seismic zone, western India, *J. Geol. Soc. India* **81,** 1–2.

Russell, D. R. (1987). Multi-channel processing of dispersed surface waves, *Ph.D. Thesis*, St. Louis University, St. Louis, Missouri.

Sabra, K. G., P. Gerstoft, P. Roux, W. A. Kuperman, and M. C. Fehler (2005). Extracting time-domain Green's function estimates from ambient seismic noise, *Geophys. Res. Lett.* **32,** doi: 10.1029/2004GL021862.

Shapiro, N. M., and M. Campillo (2004). Emergence of broadband Rayleigh waves from correlations of the ambient seismic noise, *Geophys. Res. Lett.* **31,** L07614, doi: 10.1029/2004GL019491.

Shapiro, N. M., M. Campillo, L. Stehly, and M. H. Ritzwoller (2005). High-resolution surface wave tomography from ambient seismic noise, *Science* **307,** 1615–1618.

Tandon, A. N. (1973). Average thickness of the Deccan Traps between Bombay and Koyna from dispersion of short-period Love waves, *Pure Appl. Geophys.* **109,** 1693–1699.

Wessel, P., and W. H. F. Smith (1998). New, improved version of Generic Mapping Tools released, *Eos Trans. AGU* **79,** no. 47, 579.

Koyna Project
Council of Scientific and Industrial Research (CSIR)–National Geophysical
Research Institute
Uppal Road
Hyderabad 500007, India
sunil.rohil@gmail.com
    (S.R., N.P.R., D.S., H.V.S.S.)

Scripps Institution of Oceanography
University of California, San Diego
9500 Gilman Dr
La Jolla, California 92093-0238
    (P.G.)